

# PHYSICS NEWS

BULLETIN OF THE INDIAN PHYSICS ASSOCIATION

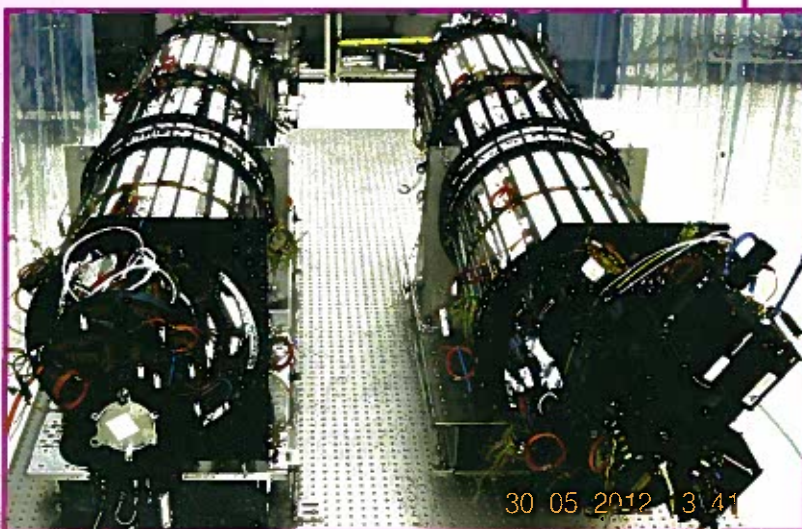
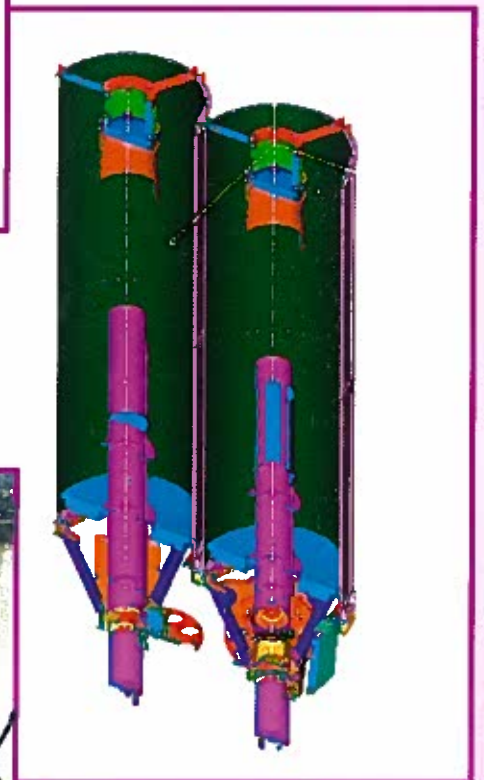
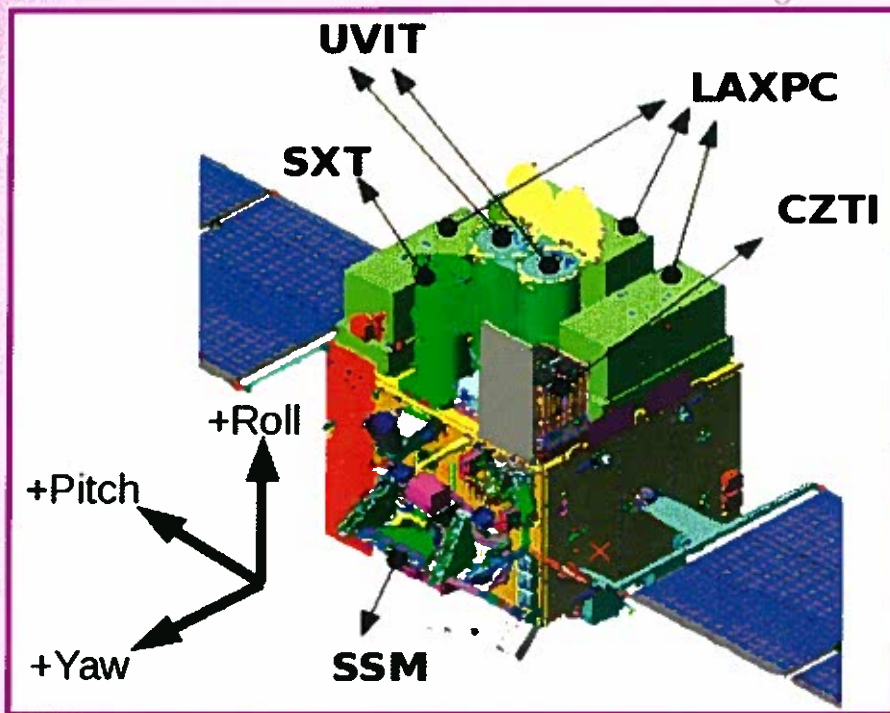
[www.ipa1970.org.in](http://www.ipa1970.org.in)

July - December 2016

Nos. 3-4

Vol. 46

ISSN : 0253 - 7583



"Instruments and Telescopes on board ASTROSAT" (photo courtesy : ISRO and UVIT Team)

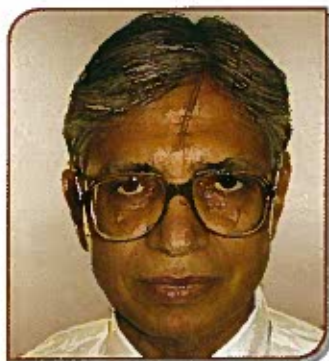
# ASTROSAT – Indian Multiwavelength

## Astronomy Satellite to View the Invisible Universe

**P. C. Agrawal**

**UM – DAE Center for Excellence in Basic Sciences :**

**Mumbai University Campus at Vidhyanagari, Mumbai - 400098**



P.C. Agrawal joined TIFR in 1962 and his research interests are mainly in X-ray Astronomy using Balloon, Rocket and Satellite borne instruments. After his Ph.D. he joined California Institute of Technology, Pasadena as a post-doctoral Research Fellow and contributed to the development of HEAO-1 A2 experiment during 1972-75. He was later a NASA/NRC Senior Research Associate at Jet Propulsion Laboratory and at NASA Marshall Space Flight Center. He has made extensive research contributions in X-ray astronomy and to the development of detectors for space missions. He was originator of the proposal for Indian Multiwavelength Astronomy satellite known as ASTROSAT and was its Principal Investigator (PI) during 2001 – 2011. He and his group at TIFR were mainly responsible for the

development of LAXPC instrument on ASTROSAT. He is at present associated with UM-DAE Center For Excellence In Basic Sciences.

### Introduction

Since his appearance on the earth, man has looked at the sky and wondered about the myriad shining objects during the night. What are these shining stars, what makes them shine, where are they located and similar other questions had haunted human mind since ages. With about 5 mm size pupil, human eye can detect ~2000 stars in the night sky. While most stars appeared constant in the sky, many of them appeared to change brightness. On rare occasions, suddenly a bright new star termed as 'guest star' or 'Nova' appeared in the sky. One such spectacular event was recorded by Chinese court astronomers in the year 1054 AD. It was so bright that it became visible even in the day for 23 days and then over the next 600 days it grew dimmer and dimmer and slowly faded away. Danish astronomer Tycho Brahe detected a similar new bright star in the year 1572 and German astronomer J. Kepler also recorded appearance of a bright new star in 1604.

The mystery of these guest stars now known as 'Supernovae' was solved only several hundred years later. Invention of Optical telescope by Galileo in 1609 revolutionized astronomy as the dimension of the observable universe expanded dramatically from our Solar system and nearby stars to dimmer stars in distant reaches of the sky. As the size of the telescopes grew over next 400 years, man could observe fainter and farther objects leading to the landmark discovery of "Island Universes" (or Galaxies like our Milky Way) and expansion of the Cosmos by Edwin Hubble in 1920's with the newly set up 100 inch aperture reflecting telescope at Mount Wilson in USA. Observations with the 200 inch Hale telescope at Mount Palomar in California (USA) unraveled mystery of peculiar star-like objects (now known as Quasars) that showed large shift in wavelength of their spectral lines towards red part of the spectrum (this is known as Red Shift) in 1963. The red shift was interpreted as

arising due to high recession velocity of the radiating objects and this implied that they are at distances of several hundred million light years. Discovery of Quasars expanded the horizon of the universe that could be probed to farther and farther regions meaning earlier and earlier epochs of its evolutionary history.

### Invisible Universe

Till 1945 all our knowledge about the universe came from a small part of the electromagnetic spectrum in 350 nm to 600 nm band visible to the human eye. The electromagnetic spectrum extends from long wavelength radio spectrum (~ MHz to 1000 GHz) to shorter wavelength radiation in Infrared, Ultraviolet, X-ray and Gamma-ray bands as shown in figure 1.

The earth is surrounded by a thick envelope of atmosphere equivalent to ~ 1000 g/cm<sup>2</sup> of water that blocks out major part of the electromagnetic spectrum. Before the advent of the space age all our knowledge of the universe came from observations

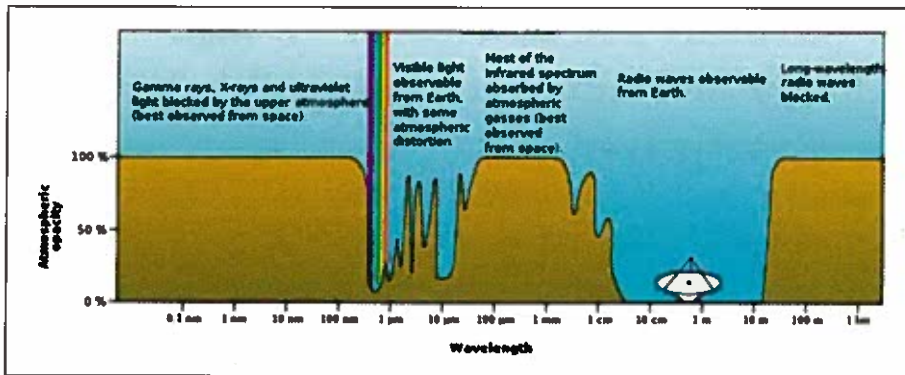


Fig 1: Transmission of electromagnetic radiation at different wavelength through earth' atmosphere (from Wikipedia).

made from the earth based studies. Chance discovery of radio emission from the Center of the Milky Way by Karl Jansky in 1930s opened up the radio waveband for the exploration of the universe and marked the birth of Radio Astronomy. A bright radio sources discovered in 1948 named as Taurus A, was found at the position of a nebular object of about 8<sup>th</sup> magnitude (Magnitude is a logarithmic scale to measure brightness of celestial objects, a difference of 5 magnitudes implies a difference in brightness by a factor of 100) detected for many decades by astronomers at the position of the guest star recorded by Chinese in 1054 AD. This bright nebulosity has filamentary structure which was imagined to be like image of Crab and hence this object came to be known as Crab Nebula. Multi-wavelength Images of the Crab nebula are shown in Fig. 2.

After the Sun it is the most extensively studied stellar object in the universe radiating from radio band to GeV and TeV (1 TeV = 10<sup>12</sup> eV) gamma-rays and has proven a gold mine of astrophysical knowledge. These objects known as Supernova remnants result from massive stars that undergo violent explosions at the end of their evolution when they had exhausted all their nuclear fuel. Radio emission and optical counterparts of

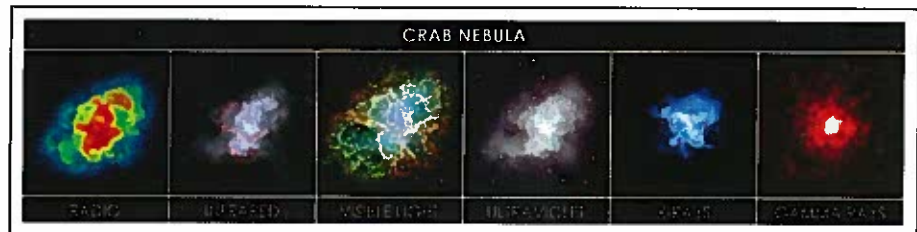


Fig 2 : Images of Crab Nebula, remnant of stellar explosion of 1054 in different spectral bands ( from Wikipedia).

the events of 1572 and 1604 were also discovered and are now called Tycho's SNR and Kepler's SNR. Advent of 'Space Age' in 1957 with the launch of first man made satellite Sputnik led to the development of Satellite based Observatories opening up studies in Ultraviolet (100-320 nm, X-ray (100 eV to 100 keV), and Gamma-ray (~ 100 keV to 100 GeV) windows to probe 'Hot Universe' and high energy processes in the cosmic sources. High temperature plasma in the outer layers of stars (stellar coronae), accretion processes in white dwarfs, neutron stars and black holes in binaries lead to formation of hot accretion disks around them that emit X-rays and UV radiation copiously. Similarly AGNs whose central engine is a massive accreting black hole, emit radiation in UV and X-rays from the accretion disks around the black hole. The launch of UV satellite ANS (Netherlands Astronomy Satellite) followed by IUE (International Ultraviolet Explorer) in 1978 and

GALEX (Galaxy Ultraviolet Explorer) in 2003 enabled imaging and spectroscopic observations in the UV band and led to major advances in understanding of origin of UV emission from all classes of cosmic objects.

Compton Gamma-ray Observatory discovered a few thousands Gamma-ray Bursts (GRBs), considered as the most violent explosive events in the universe resulting from mergers of neutron stars or black holes. Launch

of Fermi gamma-ray mission with LAT (Large Area telescope) having order of magnitude better sensitivity in 2006, transformed gamma-ray astronomy with detection of about 2000 discrete gamma-ray sources, a majority of them AGNs. Radiation mechanisms generating gamma-rays of ~ 0.1 GeV to ~ tens of TeV are the most energetic processes in nature involving production, acceleration and collisions of protons and electrons of ~ 10<sup>10</sup> - 10<sup>17</sup> eV. These are the most powerful natural accelerators in the universe.

### Birth of X-ray Astronomy and Early Discoveries by the X-ray satellite UHURU

A US scientist Riccardo Giacconi and his colleagues working at a US company called American Science & Engineering (AS&E) and well known cosmic ray physicist Bruno Rossi at MIT launched on June 12, 1962 a spinning rocket experiment with two pan cake shaped Geiger-Muller counters to study lunar X-rays. No X-

rays were detected from the Moon but instead a bright source of X-rays was detected from the direction of Scorpius constellation. Detailed analysis of the data led to the conclusion that it is an extra-solar X-ray source now known as Scorpius X-1 or Sco X-1 which is even now the brightest X-ray object in the sky (Giacconi et al. 1962). This discovery was soon confirmed independently by another rocket experiment carried out in April 1963 by scientists of Naval Research Laboratory (NRL) who also discovered in the same experiment that Crab Nebula is a bright X-ray source (Bowyer et al. 1964). Thus X-ray astronomy was born in 1962 and for this epoch making discovery R. Giacconi was awarded Nobel Prize in Physics in 2002 on the 40<sup>th</sup> anniversary of the discovery of first extra-solar cosmic X-ray source.

The nature of Sco X-1 and its X-ray production mechanism remained a mystery for a long time. Is it a star-like object or an extended source like Crab Nebula? AS&E-MIT group conducted another rocket experiment in 1964 to measure location and size of Sco X-1 precisely and found that the size of Sco X-1 was < 7 arc-sec. Observations at the location of Sco X-1 revealed presence of a 13<sup>th</sup> magnitude star. From X-ray spectral data and distance estimate X-ray luminosity of Sco X-1 was calculated to be  $\sim 10^{36}$  ergs/sec which is about 1000 times its optical luminosity and therefore Sco X-1 is truly an X-ray star. This was an extraordinary finding as no other celestial object of this type was known. What is the energy source for this prodigious rate of X-ray emission? Nuclear fusion and rotational energy loss as inferred in the case of Radio Pulsars discovered in 1967, were ruled out. Russian astrophysicist I.S.S. Shklovsky

(1967) made a bold suggestion that this huge energy can originate from in-fall of matter in the deep gravitational potential well of a neutron star from a normal companion star in a binary system. But this idea did not receive wide acceptance. The energy source of Sco X-1 and other X-ray bright sources remained elusive till the advent of UHURU satellite on the scene.

AS&E group developed large area ( $\sim 800 \text{ cm}^2$ ), low background rate proportional counters equipped with mechanical collimators of  $5^\circ \times 5^\circ$  and  $5^\circ \times 0.5^\circ$  field of view, which were launched aboard the first X-ray astronomy satellite named UHURU on December 12, 1970. After its launch UHURU scanned several times across a known X-ray star Centaurus X-3 in 1971 and discovered that its X-ray intensity was changing regularly

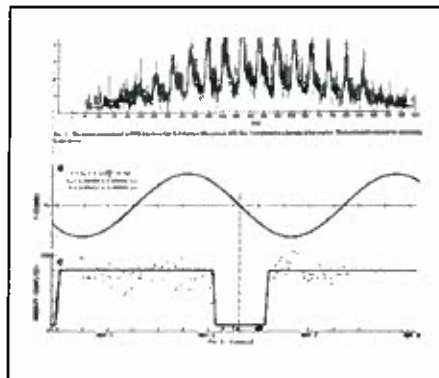


**Fig 3 : Discovery of 4.8 sec X-ray pulsations and binary nature of Cen X-3 (Giacconi et al. 1971, Schreier et al. 1972).**

with 4.82 sec period which was varying with 2.08 day period in a sinusoidal fashion as shown in figure 3. More observations revealed presence of X-ray eclipses with the same 2.08 day period (Giacconi et al. 1971, Schreier et al. 1972).

They correctly interpreted the 4.82 sec intensity variations as pulsations caused by spinning of a neutron star and 2.04 day period as the binary

period of the system. The periodic shift in the pulsation period is caused due to Doppler shift resulting from the revolution of the neutron star in a near circular orbit around center of mass of the binary. Optical observations of Cen X-3 field immediately showed that its optical companion is a massive O type star from which matter is fed to the neutron star. Discovery of another X-ray pulsar Hercules X-1 pulsating with 1.24 sec period and 1.8 day binary period and its optical companion star HZ followed soon afterwards. These discoveries established the dominant role of 'accretion' process. Matter falling freely on the surface of a compact object like a neutron star, gains kinetic energy due to very high gravitational potential of these stars and this gets converted to radiation by several processes operating in the sources. Accretion plays a central role in producing X-rays from Binary X-ray stars, AGNs etc.

UHURU made path breaking discoveries in X-ray astronomy and detected X-ray from almost all types of galactic and extragalactic objects. One of the popular units of expressing X-ray flux of a source is UFU (UHURU Flex Unit, 1 UFU being equal to  $1.7 \times 10^{-11}$  erg/cm<sup>2</sup>-sec in 2-6 keV).

### **Growth of X-ray Astronomy and its Current International Scenario**

The success of UHURU was followed by the development and launch of several X-ray satellite missions by NASA, ESA, U.K. and Japan in the 1970-90 era mainly with non-imaging detectors like PCs, scintillation counters etc. These missions carried out detailed studies of timing and spectral behavior of individual sources and greatly contributed to an understanding of the nature of X-ray

sources and their radiation processes. Based on the measurements of characteristics of binary sources like spin and orbital periods, X-ray luminosities etc. a model of accreting neutron star binaries was developed which has been quite successful in explaining the broad features of the binaries (Ghosh and Lamb, 1979). Accretion takes place on a neutron star having strong dipole magnetic field ( $10^{12} - 10^{13}$  Gauss) at its magnetic poles. If the magnetic axis is not aligned with its rotation axis, as shown schematically in figure 4,

confined in the accretion column, radiates X-rays by thermal and non-thermal processes. High magnetic fields lead to formation of Cyclotron features in the X-ray spectra of neutron star binaries due to quantization of orbits of electrons gyrating in the accretion column. Detection and study of cyclotron features and measurement of their energy, provides a powerful method of directly measuring magnetic fields of neutron stars in accreting binaries. Indeed a Cyclotron feature was detected in Her X-1 in at  $\sim 40$  keV

followed by German X-ray imaging satellite ROSAT which carried out the first X-ray survey of the sky with an X-ray imaging telescope in 0.1 – 2keV resulting in detection of more than 100,000 X-ray sources. Development of large format X-ray CCDs in late 80's was another major advancement in X-ray astronomy. Modest cooling requirement, about  $-100$  degree C and energy resolution of about 125 eV at 6 keV, made CCD as the focal plane detector of choice in X-ray imaging telescopes. X-ray CCD was first used in the Japanese X-ray satellite ASCA that significantly advanced X-ray spectroscopy of cosmic sources. Strong evidence for the existence of massive black holes at the center of AGNs was first provided by detection of a relativistically broadened and asymmetric 6.4 keV fluorescent iron line in the spectrum of Seyfert galaxy MCG-6-30-15- by ASCA (Tanaka et al. 1995).

In 1999 NASA launched Chandra X-ray observatory (CXO) with larger area and vastly improved X-ray mirrors and focal plane X-ray detectors sensitive in 0.1 – 10 keV that has unprecedented angular resolution of 0.5 arc second. Chandra has revolutionized X-ray imaging producing spectacular X-ray images of all types of cosmic objects and astronomical phenomena. In the same year ESA launched XMM-Newton (X-ray Multi-Mirror-Newton) telescope with larger reflecting area mirrors but angular resolution of  $\sim 5$  arc sec with emphasis on X-ray spectroscopic studies with CCD and dispersive X-ray devices. Japanese satellite SUZAKU, an improved version of ASCA launched in 2006 is also operational. All these observatories are sensitive in 0.1 – 10 keV and are not designed for fast timing studies.

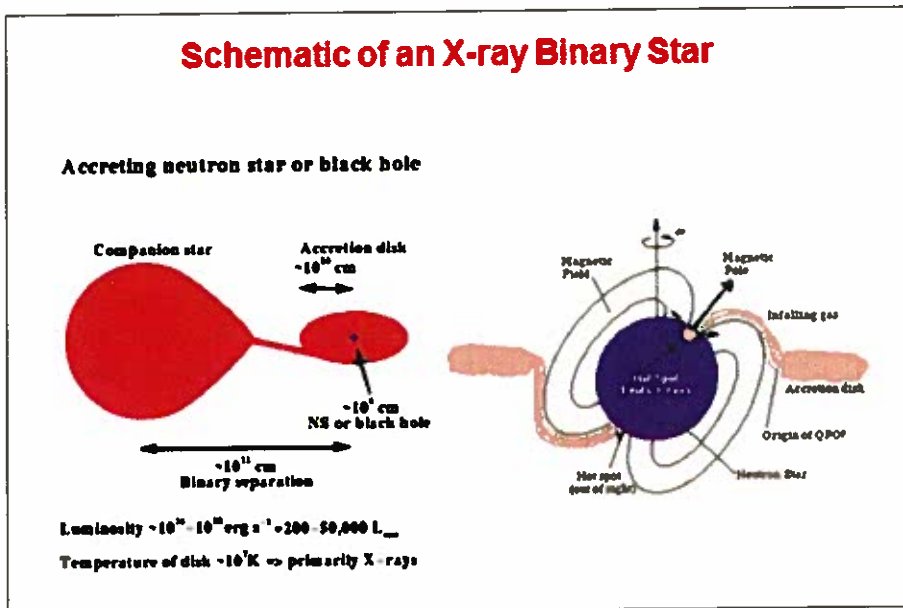


Fig 4 : Schematic diagram showing accretion of matter onto a neutron star or a black hole from its companion star. (Taken from internet, source unknown)

X-ray pulsations are observed. Matter accreting from the companion has angular momentum and hence it orbits around the neutron star resulting in formation of an 'Accretion Disk' around it. The ionized matter in the accretion disk is guided by the magnetic field lines to the magnetic poles of the neutron star resulting in formation of 'Accretion Column' above them. Matter gravitationally falling at the magnetic poles gains huge energy due to  $\sim 10$  km radius of the neutron star, being as much as  $0.1 mc^2$ . Plasma

which gave estimate of its  $B \sim 2 \times 10^{12}$  Gauss (Trumper et al, 1978). An accretion disk model developed by Shakura and Sunyaev (1973) for black hole binaries is broadly able to explain their broad features. Giacconi and Rossi (1960) had proposed the concept of a grazing angle reflecting X-ray telescope based on which X-ray reflecting mirrors were developed and launched aboard the Einstein X-ray Observatory (EO) in 1978. This led to a quantum jump in sensitivity for detection of very distant objects like AGNs. EO was

There are 2 other satellites namely International Gamma-ray Laboratory (INTEGRAL) launched by ESA in 2002 and SWIFT observatory of NASA launched in 2004. SWIFT was designed with the objective of detection, localization and temporal and spectral studies of GRBs. Both make use of coded aperture masks placed above arrays of Cadmium-Telluride (CdTe) detectors in INTEGRAL and Cadmium-Zinc-Telluride (CZT) in Swift for timing and spectral measurements. Their low energy thresholds are about 15 keV and hence they miss most of the X-ray flux. Rapid variability studies of X-ray sources are therefore difficult with them.

### **Importance of Timing Studies in X-ray Astronomy, Contributions of RXTE-PCA and Role of ASTROSAT for Timing Studies**

Among all the spectral bands, the most rapid and intense variations are detected in the X-ray region on time scales from fraction of millisecond to secs, days and months. These intensity variations may be periodic pulsations due to spin of the neutron star, binary period related modulations etc. or irregular variations due to chaotic variability from accretion instabilities, thermonuclear bursts on the surface of neutron star in Low Mass X-ray Binaries (LMXBs), quasi-periodic oscillations etc.

Most of the X-ray satellites before 1996 carried proportional counters with typical area of  $\sim 1000 \text{ cm}^2$  and had limited time resolution capability.

This changed with Rossi X-ray Timing Explorer (RXTE) launched by NASA in December 1995 with Proportional Counter Array (PCA) of 5 detectors of  $\sim 6000 \text{ cm}^2$  area and had high counting rate and micro second

time resolution capability. This brought about a qualitative transformation in timing studies as now it became possible to study very rapid variations on sub-millisecond scale. Prominent discoveries made by PCA include several hundred Hz to kHz oscillations in LMXBs, Low and high frequency Quasi-periodic oscillations (QPOs) in black hole sources, accreting millisecond X-ray pulsars, new transients etc. After working for more than 15 years during which it produced several trail blazing discoveries, RXTE-PCA ceased operation in 2012 and since then there has been no mission of comparable capability.

This gap has now been filled by recently launched Indian satellite ASTROSAT. The LAXPC instrument on this satellite, designed and developed by a team led by this author, consist of 3 identical Large Area X-ray Proportional Counters (LAXPCs) with total effective area of  $\sim 6000 \text{ cm}^2$  below 20 keV and about  $5000 \text{ cm}^2$  at 50 keV making it the largest area instrument on any mission in 3- 80 keV. LAXPC also has  $\sim 10$  micro-sec time resolution capability with high detection efficiency up to 80 keV. ASTROSAT-LAXPC with its high count rate capability and fine time resolution is expected to make major contributions to rapid variability (sub-millisecond) phenomenon.

### **Indian Contributions in X-ray Astronomy and Evolution of the concept of ASTROSAT**

X-ray astronomy studies in India began in 1967 with balloon and rocket-borne detectors at Tata Institute of Fundamental Research (TIFR), Mumbai and independently at Physical Research Laboratory, Ahmedabad. The experiments at

TIFR were initiated by Prof B.V Sreekantan who had participated in USA in AS&E- MIT rocket experiments to measure position and size of Sco X-1. The first balloon experiment, carried out in 1968 using a  $100 \text{ cm}^2$  area collimated Sodium Iodide detector from Hyderabad in India, measured rapid flux variations in Sco X-1 above 20 keV and also detected a flat non-thermal component above 50 keV in its energy spectrum. A series of balloon experiments were carried out in quick succession to measure time variability and spectra of Cygnus X-1 and other bright sources. These experiments revealed rapid X-ray flux variations and occurrence of X-ray flare in Cyg X-1 and also measured its energy spectrum in 20-150 keV. These results appeared in Nature and other journals leading to international recognition of the TIFR group. Rocket experiments were also conducted by the TIFR group in 1973-85 period to study low energy X-rays from Sco X-1, Crab Nebula etc and to map the spatial and spectral distribution of hot plasma producing 0.1 – 3 keV diffuse soft cosmic X-ray background. Advent of several X-ray satellites after 1975 equipped with instruments of better sensitivity and providing long observation time, made balloon and rocket experiments in X-ray astronomy scientifically unviable by mid-eighties.

The TIFR group, jointly with the astronomy group at ISRO Satellite Center (ISAC), Bangalore submitted a proposal in early 1986, with this author as the Principal Investigator (PI), to the Indian Space Research Organization (ISRO) for 'An Indian X-ray Astronomy Satellite' for study of time variability and spectral characteristics of cosmic X-ray sources. The X-ray payload named as

Indian X-ray Astronomy Experiment (IXAE), with three identical Pointed Proportional Counters (PPCs) of  $3^\circ \times 3^\circ$  field of view and total effective area of  $1200 \text{ cm}^2$ , was developed in a record period of 18 months and launched aboard Indian Remote Sensing satellite IRS-P3 on March 21, 1996. In 800 km polar orbit the charged particle background at higher latitudes ( $> 50^\circ$ ) is very high and useful data can be obtained for only about 20 minutes in an orbit. Being a remote sensing mission the IXAE was allotted 2 months in a year for pointing at the sky to observe X-ray sources. The IXAE worked well for  $\sim 5$  years and ceased operation when it could no more be pointed at the sky. Despite all the above limitations IXAE studied pulsations, binary period, QPOs, and erratic variability of several X-ray binaries. IXAE was among the first experiment to make detailed and long observations of the now well-known black hole binary GRS 1915+105 discovering QPOs and Quasi-periodic intense X-ray bursts of  $\sim 50$  sec period shown in figure 5 from Paul et al. 1998. This enigmatic object called a Micro-quasar was studied around the same time with PCA on RXTE and similar results were obtained. The quasi-regular X-ray bursts have been termed now as 'the heart beats of a black hole'.

Success of the IXAE was a great morale booster and it gave confidence that we can design and develop X-ray detector systems that will work in the harsh environment at the satellite altitudes. This author submitted a proposal in 1996 to Director of TIFR with a copy to Dr. K. Kasturirangan, then Chairman of ISRO for an Indian satellite experiment for 'Study of the X-ray Sky in 2-80 keV with Large Area Xenon-filled Proportional Counters'.

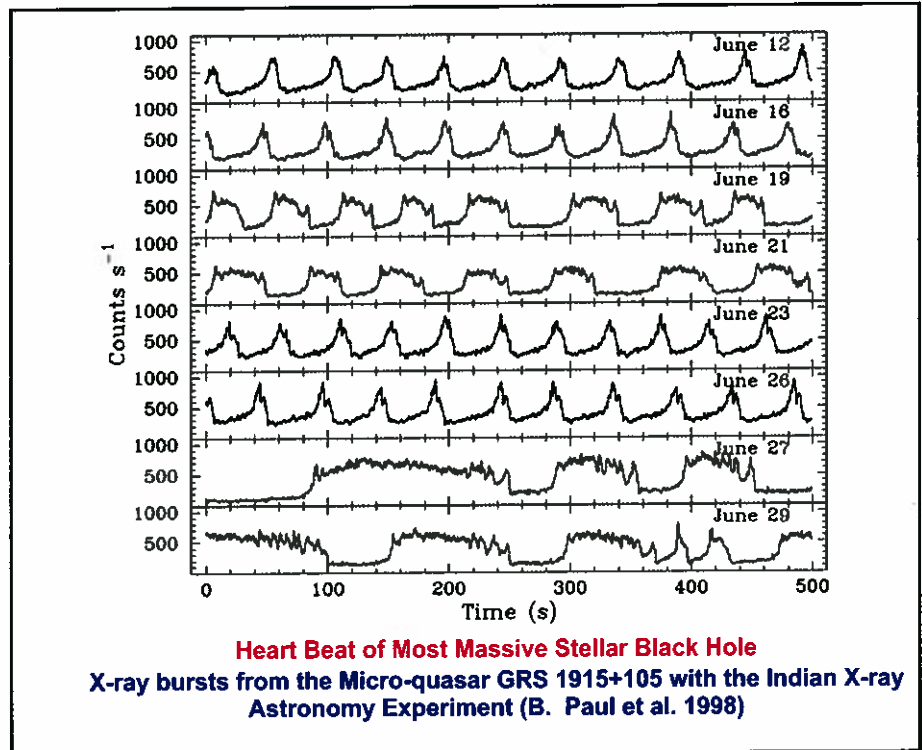


Fig 5 : Quasi-regular bursts from the Black hole binary GRS 1915+105

ISRO Chairman suggested convening a meeting of Indian astronomers at ISRO Hq. to have wider discussion of this proposal as well as other ideas and proposals that may be put forth. The meeting held in July 1996, discussed various ideas and proposals by the participants following which the Chairman constituted 2 working groups to recommend most suitable instruments for the proposed satellite. After intensive deliberations spread over two years, the groups converged on the principal science goals of the mission and the instruments required to achieve them. It was agreed that the focus of the mission will be on timing and spectral measurements in 0.3keV to 100 keV X-ray band by simultaneous observations with co-aligned X-ray instruments supplemented by simultaneous Ultraviolet (UV) observations with a co-aligned UV telescope. This broad spectral coverage gave ASTROSAT a unique

distinction of a Multi-wavelength observatory unlike any other astronomy mission. A detailed proposal of ASTROSAT with technical details was submitted in May 2000. This author submitted the proposal as its PI on behalf of consortium of participating institutions led by TIFR that included ISRO Satellite Center (ISAC) and Indian Institute of Astrophysics (IIA), Bangalore. At a meeting convened by the Chairman ISRO at TIFR in September 2000 attended by the leading astronomers and other scientists of the country, science justification of ASTROSAT, expected new science and capability of participating institutions to realize the science instruments, were discussed at length. The meeting strongly supported the concept of ASTROSAT as it felt that this mission had potential of propelling India to the forefront of research in frontier area of High Energy Astrophysics. Subsequently the ASTROSAT

proposal was approved by Space Commission and it provided seed money for developmental work on the science instruments. To ensure that science instruments are developed meeting the scientific and technical specifications, an 'ASTROSAT Progress Monitoring Committee (APMC)' under the chairmanship of Dr. George Joseph, a distinguished space scientist, was set up by the Chairman ISRO. Prof. G. Srinivasan, a member of APMC, played an important role in the initiation and development of the ASTROSAT. The APMC met periodically several times in a year, critically reviewed the progress of development of the payloads and provided valuable guidance in resolving various technical issues that arose from time to time.

### **ASTROSAT Science Goals, Strategy and Considerations in Selection of Science Instruments**

During the course of discussions in the science working groups it was agreed that configuration of ASTROSAT instruments should be so chosen that it will be a unique mission with a capability in niche areas. The following considerations and science drivers governed the selection of the payloads for ASTROSAT:

- (1) It should have a broad spectral coverage in X-rays so that timing and spectral characteristic of X-ray sources can be measured at any given time in  $\sim 0.3$  -100 keV range using more than one co-aligned X-ray instruments. Simultaneous measurements over about 3 decades in X-ray energy were essential to disentangle complex multi-component energy spectra of cosmic sources.
- (2) Study of intensity variations over time scales of milliseconds and sub-milliseconds requires high counting rate capability not only below 20 keV but also up to  $\sim 100$  keV. This in turn requires large area X-ray detectors having high detection efficiency up to 100 keV. The X-ray instrument should have high time resolution ( $\sim 10$  microseconds) capability to measure the arrival time of each photon.
- (3) Most existing X-ray astronomy missions work in a specific limited spectral band and thus there is a lack of capability in making simultaneous observations in many spectral regions. Study of sources from a single space platform in the multiple spectral bands is essential to decipher the true nature of the cosmic sources. In principle MW studies of any target object should be possible by coordinated simultaneous measurements from several space observatories. Since observatories are in widely different orbits and have varying operational constraints, the coordinated observations pose serious logistical challenges resulting only in limited success. To fill this lacuna ASTROSAT was planned to be a Multi-wavelength Observatory that covers X-ray as well as UV spectral bands.
- (4) Optical astronomy community in India had wide interest in UV studies of a variety of stellar and extra galactic sources. Inclusion of a sensitive Ultraviolet Imaging Telescope(UVIT) with angular resolution of  $\leq 2$  arc sec on ASTROSAT, will fulfil this need and that of MW observations. Planned twin telescope of UVIT with 38 cm mirrors will be a significant improvement over the Galex mission launched by NASA in 2003.
- (5) Since the X-ray sky is highly variable, an X-ray Sky Monitor similar to the ASM instrument on RXTE, was planned to monitor the X-ray sky continuously.
- (6) During the course of its orbit a satellite passes through a zone of high fluxes of protons and electrons, known as South Atlantic Anomaly (SAA) region. A small Charged Particle Monitor (CPM) was included on ASTROSAT to provide alert to the X-ray detectors for switching off in zones of high flux of particles.

Additionally following considerations were kept in mind for the selection and design of the instruments:

- (a) The main X-ray instrument with high count rate and time resolution capability should be based on well proven technology in which we have experience and expertise to design and develop it indigenously. It should be a multi-detector system to provide redundancy. Large Area Proportional Counter (LAXPC) with 3 identical units, each fully independent with own HV and electronics, was chosen as TIFR X-ray group had long experience in the design and operation of such detectors.
- (b) An instrument covering 0.3 – 8 keV is important for accurate measurements of continuum and line spectra. This is achieved by a conical foils based X-ray mirror with an X-ray CCD as the focal plane detector, to provide angular resolution of a few arc minutes and energy resolution of 2 to 3% at 6 keV. Development of X-ray



reflecting optics based imaging instrument named as Soft X-ray Telescope (SXT), was a new technological challenge that was taken up by TIFR. An agreement was reached with University of Leicester (UoL), U.K to fabricate CCD Camera for the SXT and in return providing 3% of observing time on ASTROSAT to UoL.

- (c) New generation of pixelated hard X-ray detectors like Cadmium Telluride (CdTe) and Cadmium-Zinc -Telluride (CZT) have advantage of high detection efficiency up to hundred keV, can be made into a large array of pixels and with a Coded Aperture Mask (CAM) to provide low resolution imaging in 20-100 keV. A CZT Imager (CZTI) to be developed by TIFR, was included on ASTROSAT.
- (d) Design of X-ray sky monitor on ASTROSAT, named as Scanning Sky Monitor (SSM), makes use of 3 units of one dimension position sensitive proportional counters sensitive in 2-10 keV, equipped with CAM to measure position of sources to accuracy of  $\sim 0.1-0.2$  degree. This development was taken up by ISAC, Bangalore.
- (e) Design and development of UVIT posed a major challenge as no prior experience or expertise was available in India for the making UV optics or photon counting UV imaging focal plane detectors. ISRO's Laboratory for Electro Optics System (LEOS) agreed to take up fabrication of primary and secondary mirrors of UVIT. An offer from Canadian Space Agency (CSA) to collaborate in UVIT by providing imaging detectors with associated signal processing electronics, was accepted and in turn ISRO agreed to provide 5% observing time on ASTROSAT to CSA.

## ASTROSAT Science Instruments

An early description of ASTROSAT and its science instruments can be found in Agrawal (2006) and a more recent description can be found in Singh et al.(2014). Brief description of the instruments and their characteristics is presented in the following sections:

### (I) Large Area X-ray Proportional Counter (LAXPC) Instrument:

LAXPC is an entirely indigenous instrument all the components of which have been designed, developed and fabricated by the TIFR group. It consists of 3 identical multi-anode, multilayer proportional counters (PCs) having 100 cm X 36 cm X 15 cm X-ray detection volume. This is achieved by 60 Anode cells, each with a 37 micron diameter gold

sides and bottom of the detector. The adjacent anode cells are electrically isolated from each other by cathode walls of 50 micron diameter Be-Cu wires spaced 3mm apart.

Alternate anode cells of top two layers are linked together to provide 4 outputs. Similarly all the anode cells of layer 3, 4 and 5 are connected to provide a single output from each layer. These 7 outputs from each LAXPC are operated in mutual anti coincidence and in anti coincidence with 3 Veto layers. This ensures that only genuine X-ray events are accepted. All the detection cells mounted in machined aluminium frames are stacked up and mounted with fasteners on bottom plate of the detector housing. End view of complete Anode assembly of a LAXPC is shown in figure 6.

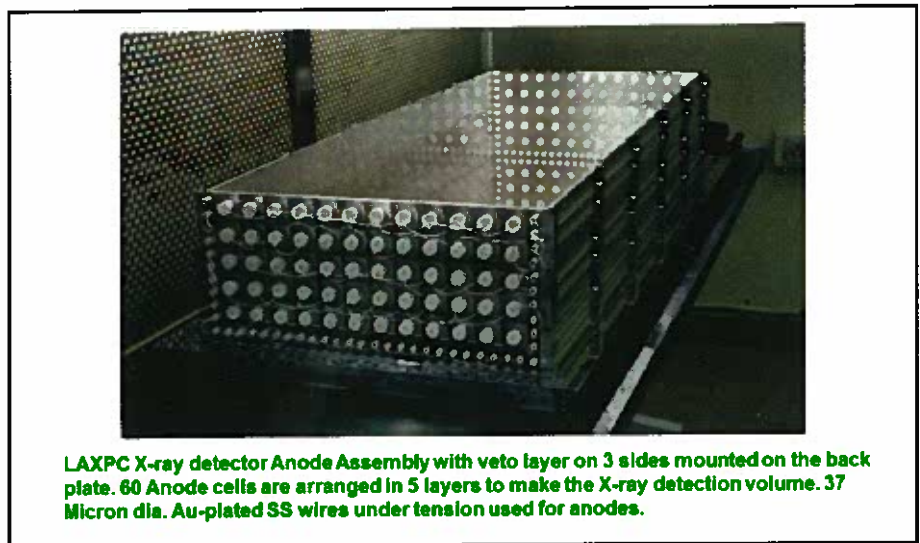


Fig 6 : End view of LAXPC detector anode and Veto layer assembly mounted on back plate of detector housing (courtesy - LAXPC team).

coated stainless steel wire, having cross-section of 3 cm x 3 cm, arranged in 5 layers. The X-ray detection anode' cells are surrounded on 3 sides by 3 Veto layers with a total of 46 Veto cells each 1.5 cm x 1.5 cm x 100 cm to reject events caused by interaction of gamma-rays and charged particles entering the detector volume from the

The Anode assembly is housed in a leak proof detector housing that is sealed at the bottom by the Back plate with Anode assembly. The top side is sealed gas tight by using a 50 micron thick Mylar film that serves as X-ray entrance window. Thin Mylar film is supported against the gas pressure by a honey-comb geometry

Window Support Collimator (WSC) made of slotted aluminium alloy slats mounted in bottom part of a collimator housing. Design and fabrication of Field of View Collimator (FOVC) with low mass but opaque to X-rays of up to 80keV entering from outside the  $\approx 1^\circ \times 1^\circ$  FOV, was a major challenge in LAXPC detectors. The FOVC is made from slats of five layers of tin, copper and aluminium glued together by epoxy. Regularly spaced slits are cut by laser

The assembled LAXPC is baked at 80°C and continuously evacuated for 3 weeks and then filled with a mixture of about 90% Xenon and 10% CH<sub>4</sub> at a pressure of 1520 torr to achieve high detection efficiency as Xe (Z=54) has large photoelectric cross-section up to 100 keV. Xenon is very sensitive to electronegative molecules like O<sub>2</sub>, OH, Halogens etc. at level of > 5 ppm as electrons get attached to these molecules causing degradation of

HV in range of about 2200 to 3000 V is supplied to anodes of each LAXPC by a command controllable compact HV unit developed at TIFR. Charge pulses of the anode layer are amplified and shaped by Charge Sensitive Preamplifiers (CSPAs) followed by a pulse stretcher. A signal processing electronics unit incorporating electronics logic accepts only events producing signal from a single cell and not accompanied by veto signal. An exception is made for those double events which result from absorption of Xenon K- fluorescent photon, in another cell. In the normal mode of operation of LAXPC, pulse height of each genuine X-ray event is measured by a 1024 channel pulse height analyzer and its arrival time also tagged to an accuracy of 10 micro-sec by a precision Signal Time Base Generator. The count rates of these events are also stored in several Broad Band Counters in selectable integration times.

Combined Effective area (geometrical area  $\times$  detection efficiency) of 3 LAXPCs is plotted as a function of X-ray energy in fig 8 along with that of RXTE/PCA for comparison. It is seen that above 20 keV LAXPC instrument will have ~ 5 times larger area than that of PCA providing it much higher sensitivity at high energies.

The LAXPCs were calibrated by shining 5.9 keV, 22.2 keV and 59.6 keV X-rays from collimated Fe<sup>55</sup>, Cd<sup>109</sup> and Am<sup>241</sup> radioactive sources respectively. The sources mounted in a moving carriage driven by a dc motor can be programmed to shine X-rays continuously or at discrete intervals along the entire area of the detector to derive average response over it. The calibration was carried out in a thermovac chamber at several



All the three LAXPC Space flight detectors in Assembly, integration and testing lab (AIT) lab after successfully completing all flight tests and final calibration (20<sup>th</sup> October 2014).

Fig 7 : The 3 LAXPC units ready for integration with the satellite after completion of all the tests (courtesy - ISRO).

in the 5 layered slats which are then crossed and assembled to make FOVC. This is mounted in the top part of collimator housing and its cells are exactly aligned with those of WSC. To block leakage of X-rays from the sides of the detector housing its 5 sides and sides of collimator, are shielded with 1 mm thick tin sheet coated with copper. Picture of fully integrated and qualified LAXPC detectors ready for integration with satellite bus at ISAC integration facility, is shown in fig 7.

energy resolution. When exposed to the atmosphere, these molecules diffuse through the thin Mylar window in the counting gas affecting energy resolution. To overcome this problem a Gas Purification unit was developed in collaboration with ISRO Inertial System Unit (IISU) and is an integral part of each LAXPC. The purifier can be activated by command in the orbit and in a few hours the entire gas volume is purified restoring resolution to normal value.

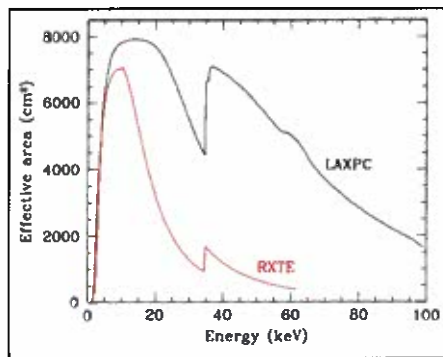


Fig 8 : Plot of Effective area of LAXPC instrument compared to that of RXTE / PCA versus Energy (courtesy - LAXPC team).

temperatures. Energy resolution of 3 LAXPCs was measured and found to be ~10 to 11% at 30 and 60 keV.

(II) Soft X-ray Imaging Telescope (SXT) :

SXT is an X-ray imaging instrument based on the use of X-ray reflecting mirrors made of gold coated aluminium surfaces shaped as sections of paraboloid-hyperboloid. X-rays incident at grazing angles ( $<1^\circ$  from the telescope axis) are reflected successively from the two gold coated surfaces and brought to the prime focus of the telescope at 2 meters to realize ~ 3 arc minutes angular resolution. The mirror assembly is made of 4 identical segments each having 40 concentric and confocal foils that constitute the paraboloid and hyperboloid mirrors. A custom made RF sputtering machine was developed and installed at TIFR for producing replicated gold surfaces subsequently deposited on the aluminium foils to fabricate several hundred mirror foils. The entire mirror assembly of 320 reflecting foils is housed in machined housing with accurately machined grooves that keep each foil mirror in designed shape. A schematic view of SXT is shown in fig 9 (a).

The focal plane detector is an X-ray CCD mounted on a multistage thermo electric cooler coupled to a

radiator plate by a heat pipe, to keep CCD at  $-80^\circ\text{C}$  to minimize thermal noise. The CCD records X-ray image and energy of each detected photon. The CCD used in SXT is a three phase frame transfer device consisting of an imaging part of  $600 \times 602$  pixels each of  $40 \text{ micron} \times 40 \text{ micron}$  size and storage part of  $600 \times 602$  pixels of size  $39 \text{ micron} \times 12 \text{ micron}$ . After exposure to X-ray source, the X-ray image is immediately transferred to storage section so that the CCD camera is

assemblies of SXT are housed in a three part tube made from Composite Fiber Reinforced Plastic (CFRP) at the bottom of which is attached FPCA. The tube entrance is covered by a mechanical door to protect X-ray optics against out gassing from various onboard instruments, and is commanded to open in the orbit.

The SXT effective area is  $\sim 130 \text{ cm}^2$  at 1 keV, drops at silicon K-edge at 2.3 keV to  $50 \text{ cm}^2$  and at 6 keV to  $20 \text{ cm}^2$ . Energy resolution of the SXT

**Schematic of Soft X-ray Imaging Telescope**

**Soft X-ray Imaging Telescope**  
using conical-foil mirrors with medium angular ( $\sim 3'$ ) and spectral ( $E/\Delta E \sim 20$  to  $50$ ) resolution in 0.3-8 keV.

**X-ray CCD mounted on Thermolectric Cooler to cool it to  $-80$  degree C**

Fig 9 : (a) Schematic of SXT (b) CCD of SXT mounted on cooler (courtesy-SXT team).

ready for another exposure. Read out time of the full CCD is 2.3 sec but a fast window mode in which  $150 \times 150$  pixel section centered on the X-ray image, can be read out in 278 ms is also an optional mode. The CCD is protected against exposure to radiation by a proton shield around it and from optical light by a thin polyimide film coated with  $\sim 500 \text{ \AA}$  thick aluminium film. A view of the CCD mounted on thermoelectric cooler is shown in fig 9 (b).

The CCD assembly is housed in an evacuated box whose door can be commanded to open in a one shot operation after deployment of the instrument in orbit. All the sub-

CCD recorded with 5.9 keV Mn-K $\alpha$  and 6.49 keV Mn-K $\beta$  lines from Fe 55 source is shown in fig 10 demonstrating resolution of 150 eV at 6 keV.

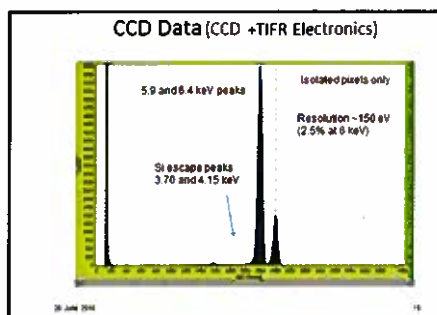


Fig 10 : Energy resolution of X-ray CCD detector at the focal plane of SXT for 5.9 keV x-rays from Iron-55 source (courtesy - SXT team).

### (III) Cadmium-Zinc-Telluride Imager (CZTI):

CZTI is a hard X-ray imaging instrument based on the use of a Coded Aperture mask (CAM) fabricated from 0.5 mm thick tantalum, placed at the entrance of the Imager above the CZT detector array to provide modest angular resolution of  $\sim 8$  arc minutes for 20-100 keV X-rays. The CZTI has geometrical area of  $1024 \text{ cm}^2$  (useful area of  $976 \text{ cm}^2$ ) consisting of 4 identical quadrants each of  $256 \text{ cm}^2$ . Each quadrant has 16 CZT modules of  $15.25 \text{ cm}^2$  useful area composed of  $2.46 \text{ mm} \times 2.46 \text{ mm}$  CZT pixels of 5 mm thickness to achieve close to 100% detection efficiency up to 100 keV. Thus there are 16384 pixels read out by 128 Application Specific Integrated Circuits (ASICs) providing position and energy of each detected X-ray. A 2 cm thick Caesium Iodide (CsI (TI)) detector viewed by a photo tube is placed below the CZT plane and operated as a veto detector to reject charged particle events and those caused by Compton scattering of higher energy photons. A collimator made from a sandwich of tantalum and aluminium restricts FOV of CZTI to  $4^\circ.6 \times 4^\circ.6$  for X-rays of up to 100 keV beyond which FOV progressively becomes wider with increasing energy. The CAM with 50% transmission, is mounted above the collimator. Shadow pattern cast by CAM depends on position of the X-ray source from the instrument axis and by measuring the shadow pattern, the source position can be derived to  $\sim 8$  arc minute accuracy. Position, energy and arrival time (1 ms accuracy) of each valid event are measured by signal processing electronics. A schematic view of CZTI and picture of fully integrated instrument are shown in fig 11.

### (IV) Scanning Sky Monitor (SSM) :

It consists of 3 identical one dimensional Position Sensitive

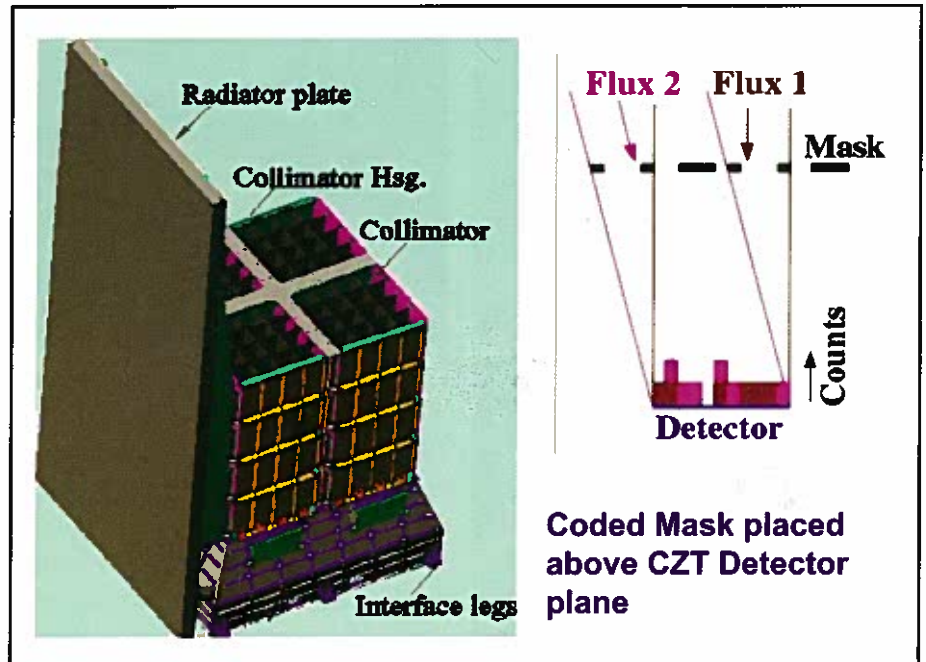


Fig 11 : Schematic view of assembled CZTI is shown on left and working of coded mask aperture is demonstrated in figure on the right (courtesy- CZTI team).

Proportional Counters (PSPCs) with FOV of  $22^\circ \times 100^\circ$ . Each PSPC has a differently coded CAM placed above the detector plane to determine position of sources in the sky using deconvolution of the shadow pattern cast by CAM. This pattern depends on the position of the source in the FOV. The position of detected photons in the PSPC is measured by 8 resistive anodes along one direction and perpendicular to it by the specific anode cell in which the signal is produced. Charge division technique is used to determine the position of interaction of photon along the resistive anodes to an accuracy of about 1 mm. This leads to an angular accuracy of  $0.2^\circ$  along the coding direction and  $2^\circ.5$  in the cross direction. The detectors are filled with Argon + Xenon + Methane gas mixture to provide high detection efficiency in 3-10 keV. The low energy threshold is due to use of 50 micron thick aluminized Mylar.

The 3 PSPCs with associated electronics are mounted on a rotating platform located on side deck of satellite as shown in fig 12. The

platform is programmed to move in discrete steps after staring at a direction for 10 minutes to scan across about half of the sky. The SSM plays important role of an X-ray 'alert' monitor.

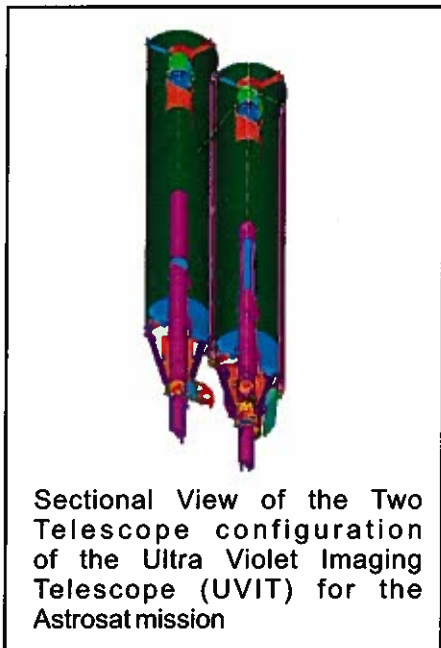
### (V) Ultra Violet Imaging Telescope (UVIT):

UVIT is a twin telescope instrument whose response covers Visible, Near - UV (NUV) and Far-UV (FUV) spectral bands. Configuration of the twin telescope UVIT is shown in fig. 13. The two almost identical telescopes are held together by a titanium cone that also serves as interface for mounting it at the center of top deck of the space craft. Each telescope has a 38 cm primary mirror and a 14 cm secondary, made from light weighted Zerodur in a Ritchey-Chretien configuration. Aluminium coating on mirrors, protected by a layer of magnesium fluoride, serves as reflecting surface. One telescope has a dichroic beam splitter to split the incoming beam into a visible band (320-550 nm) and a Near-UV (NUV) band (200-300 nm) and the second



**Assembly of SSM Detector**

**Fig 12 :** Views of individual Position Sensitive Proportional Counters used in SSM at different stages of assembly (courtesy- SSM team).



**Sectional View of the Two Telescope configuration of the Ultra Violet Imaging Telescope (UVIT) for the Astrosat mission**

**Fig. 13 :** Configuration of the twin telescopes of the UVIT instrument (courtesy-UVIT team)

telescope covers only Far-UV (FUV) spectral band (130-180 nm). Each channel has a filter wheel holding several narrow response filters through which the beam passes before reaching the detector. The FUV and NUV channel also have prism

spaced in the filter wheels for low resolution (~100) spectroscopy. The measured angular resolution of UVIT is 1.8 arc second and FOV is 28 arc minutes. Carefully designed cylindrical baffles surround each telescope to attenuate stray light from off-axis sources by a factor of ~ 10<sup>9</sup>. A photograph of the two fully



**Fig 14 :** Fully integrated two telescopes of UVIT are shown (courtesy- UVIT team).

integrated telescope with focal plane detectors in shown in fig 14.

The focal plane detectors are photon counting systems that measure the position of each photon in the image plane of the detector as well as record its arrival time. A 40 mm aperture CMOS device of 512 X 512 pixels

serves as the focal plane detector to record images. Photons reaching the focal plane pass through a MgF<sub>2</sub> window in FUV channel and a Silica window in NUV and visible channels and strike a photo cathode to produce photo electrons. The electrons are focused at the entrance of two stage Micro-Channel Plates (MCPs) which intensify the signal a million times or higher depending on the applied HV. The electrons are converted back into photons and led by a tapered fiber optic bundle to CMOS. The CMOS detector can be readout either in high gain photon counting mode, as done usually for the UV channels, or in low gain integration mode used for the visible channel.

Although the UVIT telescopes have 38 cm aperture mirrors, their effective area is ~ 10 cm<sup>2</sup> for the FUV band and about 20 cm<sup>2</sup> for the NUV channel. This is due to peak detection efficiency of ≈ 5% for FUV and ≈ 10% for NUV band. Several filters with defined transmission bands are mounted in the filter wheels and can be inserted in the paths of the beam by command for any of the 3 channels. UVIT optics and detectors are very sensitive to contamination due to out gassing from other instruments and sub-systems of the satellite. Deposition of even molecular film of contaminants may degrade optics. To prevent it, a deployable door is installed at the entrance of each telescope tube which can be commanded to open in a one shot operation in the orbit.

All the science payloads have to be qualified through stringent shock and vibration tests at levels likely to be encountered at launch. Similarly the instruments are subjected to vacuum and temperature conditions expected in the orbit by testing their performance in a thermovac chamber at different temperatures.

## ASTROSAT Spacecraft, Mission characteristics and Launch

The satellite bus for ASTROSAT is similar to that of Indian Remote Sensing (IRS) satellites with dimensions of 1.96 m X 1.75 m X 1.30 m. The 4 science instruments namely LAXPC, SXT, CZTI and UVIT are mounted on the top deck of the spacecraft with their view axes co-aligned along the roll axis of the satellite as shown in a schematic view in fig 15.

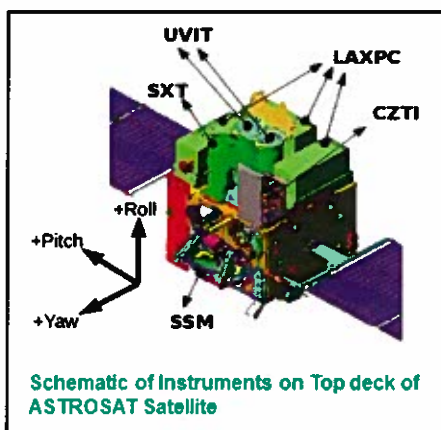


Fig 15 : Schematic view of ASTROSAT satellite with various instruments mounted on the top deck of spacecraft (courtesy - ISRO).

The SSM instrument mounted on a side panel can also be seen. Mass of the 5 science instruments is 855 kg and total mass of the fully integrated ASTROSAT satellite at launch was 1515 kg. This satellite generates ~2100 watts of power from two deployed solar panels needed to operate science instruments and other essential sub-systems. Astrosat is a 3 axes stabilized satellite that can be pointed at any target in inertial space by an attitude control system. The satellite attitude is controlled by using 3 magnetic torquers and 4 reaction wheels which get input from 3 gyros and 2 star sensors. These enable satellite to keep pointing at a specific target for long period and move satellite to other

targets in a programmed manner. The target acquisition accuracy of satellite is 3 arc minute but by using reference from star sensors it can be improved to about an arc second. Due to various perturbations in orbit the attitude slowly drifts at a rate of ~ 0.2 arc sec / sec which is continuously corrected.

The science instruments on ASTROSAT generate huge amount of science data which is stored in a 200 Gbit on board solid state recorder. A 11 m parabolic antenna at ISRO Satellite Tracking and Command (ISTRAC) facility at Byalalu is used to communicate with ASTROSAT. The data are read out in every orbit (except 3 to 4 orbits not visible over Bengaluru) by using two X-band carriers at rate of 105 MB /sec. The data recorder stores the data for the invisible orbits and all the stored data is read out in the next visible orbit. A large number of stored, time tagged and real time commands are used for the operations of the instruments and satellite systems. All the processed ASTROSAT science data are stored and archived in computers of Indian Space Science Data Center and can be accessed on-line by any user for science analysis after expiry of the proprietary period (12 months from availability of data) of a particular data.

ASTROSAT was launched on 28 September 2015 by PSLV-30 flight from Satish Dhawan Space Center in India and placed in a 650 km circular orbit with 6° inclination to the equator. The planned life of the mission is 5 years but in this orbit it can last for >10 years. After launch the science instruments were switched on one by one. ASTROSAT has been in orbit for nearly 13 months and has been making observations of various celestial sources producing new science results some of which will be presented in the next section.

First 6 months of ASTROSAT observing time are marked as Performance Verification phase to verify performance of instruments and calibrate them using known sources. The next 6 months are reserved as Guaranteed Time (GT) for the instrument teams. In the second year of operation the GT will be reduced to 50% and 35% open observing time will be available to any Indian scientist based on peer review of science merit of the proposals. In third year GT will be reduced to 30%, open time for Indian proposals will increase to 45% and 10% will be allotted for International proposals from outside India. From 4<sup>th</sup> year onwards there will be no GT for the instrument teams, 65% time is reserved for Indian proposals, 20% for international proposals and remaining time earmarked as in 3<sup>rd</sup> year.

## Preliminary Science Results from ASTROSAT

Astrosat has observed a large number of X-ray and UV bright objects in the PV phase to calibrate the instruments and also check their timing, spectral and imaging characteristics. Software for processing raw data and convert it into usable data files from which science results can be extracted are at various stages of development /completion. Results have started to emerge on some objects mainly from X-ray instruments.

Crab Nebula has been regarded as a 'standard candle' in X-ray astronomy since its flux and energy spectrum have been measured extensively in X-ray and Gamma-ray regions for more than 4 decades by almost all X-ray and Gamma-ray satellite missions. Pulsar PSR B0531+21 located in the Crab Nebula shows 33 msec pulsations over almost the entire electromagnetic spectrum and is used to calibrate timing accuracy of instruments.

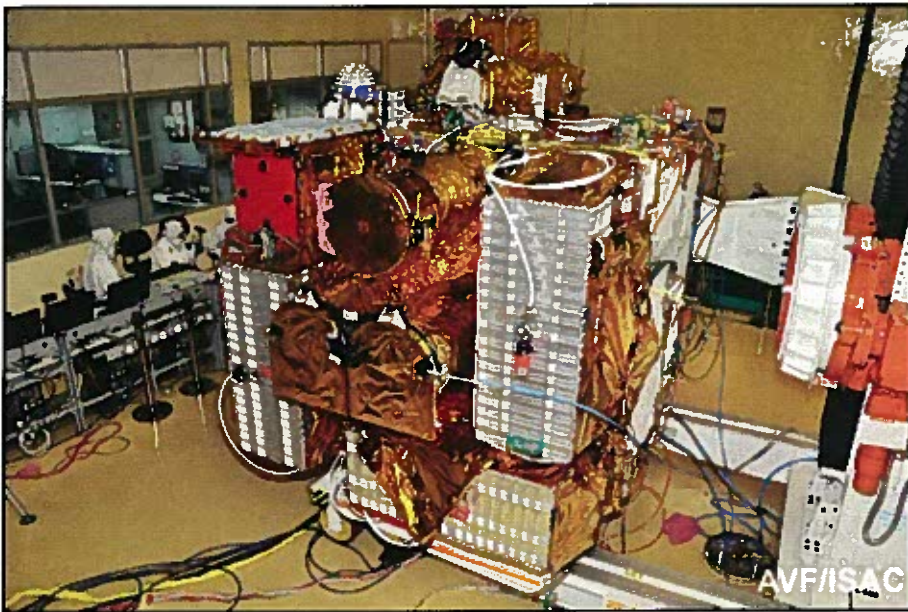


Fig. 16 : Photograph of ASTROSAT satellite with all the science instruments. The view is looking along the view axes of the instruments (courtesy-ISRO).

**(a) Preliminary Results from CZTI:** Crab Nebula was observed by CZTI on October 6 and its image in the detector plane is like that of a point source since CZTI angular resolution is  $\sim 8$  arc minutes while Crab X-ray source size in hard X-rays is  $\sim 1$  arc minute. Strong 33 msec X-ray pulsations are detected. X-ray pulse profile in 30-100 keV is shown in fig 17. Main X-ray pulse at phase 0.4 and inter pulse at phase 0.8 can be seen in the figure demonstrating normal performance of CZTI.

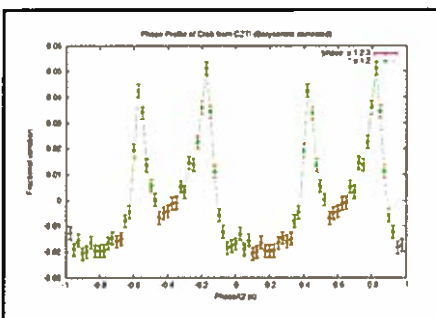


Fig 17 : 33 millisecond Pulse Profile of Crab Pulsar (courtesy - CZTI team).

An additional feature of CZTI is its ability to detect polarization of X-rays from Compton scattering of high energy X-rays (80-250keV)

from Gamma-ray bursts seen at large angles from the view axis of CZTI. GRB photons striking CZTI at large angles undergo Compton scattering in one CZTI pixel and are detected by second Compton scattering in another pixel. Since Compton scattering angle depends on polarization of Incident photon, by measuring azimuthal distribution of scattered photons one can infer

degree of polarization of the incident photons for very bright GRBs. Polarization measurement is crucial to understand radiation mechanism

of GRBs. A GRB event named as GRB151006A detected by Swift satellite was at  $\sim 60^\circ$  angle from CZTI view axis and detected as shown in fig 18. Possibility of detecting polarization from bright GRBs is promising. In the coming months more GRB results are expected to emerge from CZTI.

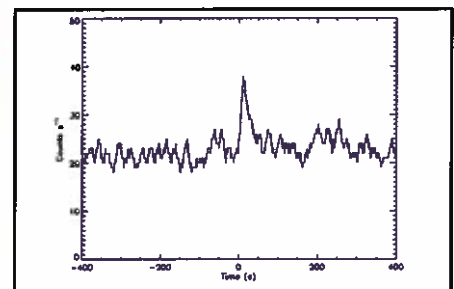


Fig. 18: Compton scattered photons from the same GRB detected by CZTI (courtesy- CZTI team)

**(b) Calibration of SSM detectors:** Bright X-ray sources like Crab Nebula, Cygnus X-1 and bright black hole binary GRS 1915+105 were observed with SSM detectors in pointed mode to check is sensitivity. SSM detected expected rate of count rates from these objects. Light curve of GRS

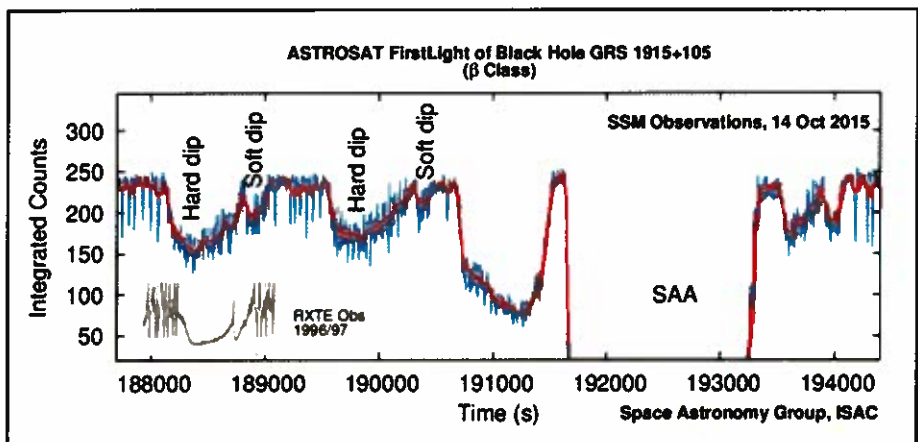


Fig. 19 : Light curve of GRS 1915+105 from pointed mode observation (courtesy-SSM team).

1915+105 is shown in Fig 19 and shows strong variability commonly observed from this enigmatic object.

It is expected that SSM will soon generate X-ray sky maps and light curves of  $\sim 100$  or more bright X-ray sources on daily basis to alert other instruments.

**(c) Early Observations by SXT:**

Among all the X-ray instruments SXT has the best angular and energy resolution but covers only 0.3-8 keV spectral band. Angular resolution of SXT was measured by pointing it at the blazar (a type of quasar) PKS 2155-304 which is a bright point-like X-ray source, on October 26, 2015. From the X-ray image of this object value of Point Spread Function was deduced as  $\sim 2.5$  arc minutes consistent with design value of  $\sim 3$  arc minutes.

The energy resolution of SXT was measured by making pointed mode observations of the young SNR Tycho A which has an 8 arc minutes size shell-like structure in radio and X-ray bands. A shock wave generated at the time of SN explosion expands and compresses the interstellar medium heating it to temperature of  $\sim 40$  million K. At this temperature, the atoms are highly ionized and produce characteristic X-ray spectral lines of different elements by recombination. The SXT observed Tycho A on November 5, 2015 and recorded its image and X-ray spectrum shown in fig 20. X-ray lines of Magnesium (1.4 keV), Silicon (1.84 keV), Sulphur (2.6 keV), Argon (2.9) and Calcium are clearly seen in the spectrum. The prominent feature at 1.84 keV is silicon line as silicon is over abundant in Tycho A. Detailed analysis of the spectrum is in progress to derive the temperature and abundances of elements. SXT has observed

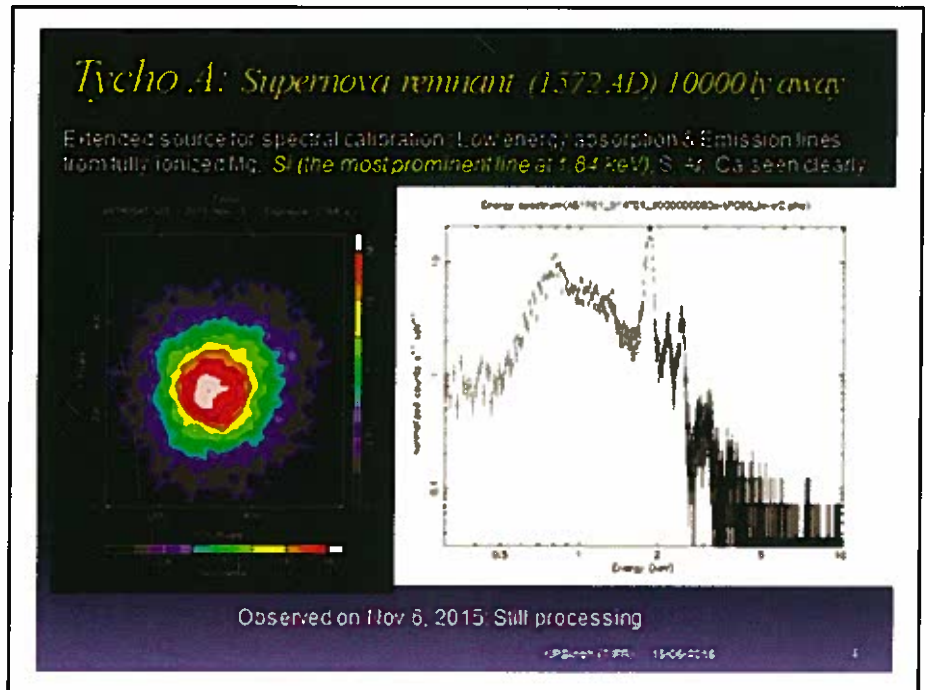


Fig. 20 : X-ray image and energy spectrum of SNR Tycho A obtained on November 6, 2015 by SXT (courtesy – SXT team).

several important soft X-ray sources that include stellar coronae, magnetic cataclysmic variables and AGNs. Analysis of the SXT data is in progress.

**(d) Calibration and initial results from LAXPC instrument:**

As discussed earlier Crab Nebula is a standard source for calibration of X-ray detectors as its characteristics like intensity and energy spectrum are well established from extensive observation in earlier missions. Hence it was chosen for calibrating the 3 LAXPC detectors. The measured Crab spectrum for LAXPC 10 unit is shown in fig 21. The red line shows the incident best fit spectrum folded with detector response and the black line connecting the observed data points is also shown. Note that due to very high count rate the errors on the data points are very small. The best fit power law has photon index  $= -2.073 \pm 0.004$  and interstellar column density ( $N_H$ ) =  $7.14 \times 10^{22}$  H atoms/cm<sup>2</sup>.

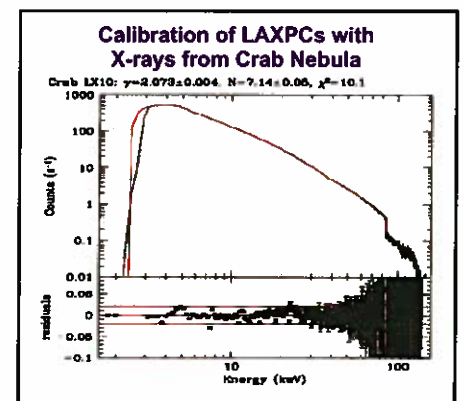


Fig. 21 : Energy spectrum of Crab Nebula measured by LAXPC 10. The best fit power law spectrum along with the data points is shown in the figure.

LAXPC instrument has observed several accreting neutron star and black hole binaries to study their timing and spectral features. Soon after turning on the HV of LAXPCs on October 20, 2015 there was a huge type II outburst of the neutron star binary 4U 0115+63 announced by an Astronomical Telegram. This High Mass X-ray Binary (HMXB) has a pulsar of 3.61 sec period which is the spin period of the neutron star and a



24.3 day binary period. The ASTROSAT instruments were therefore pointed at this binary on October 25. LAXPCs detected a very large flux from the source as shown in the counting rate plots of 3 LAXPCs in fig 22. Note that there are intensity

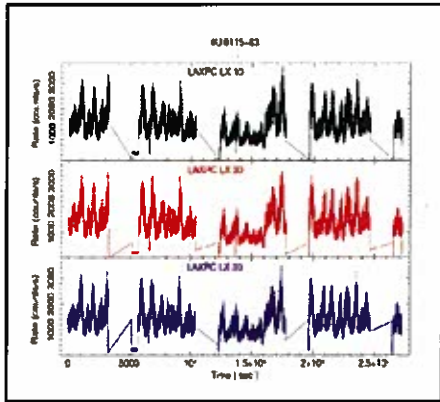


Fig. 22 : Plots of LAXPC count rates in 3-80 keV versus time for the binary system 4U 0115 +63 during its outburst on October 25, 2015 (courtesy-LAXPC team).

spikes seen in all the 3 LAXPC count rates which appear at nearly regular interval of  $\sim 1000$  sec. This intensity oscillation is a new phenomenon whose origin is not well understood but probably caused by instabilities in mass accretion rate from the disk.

Strong 3.6 sec X-ray pulsations are clearly detected in fig 23 where count rates in 0.10 sec bins are plotted against time for the 3 LAXPCs. Note that the pulsed flux is  $\sim 50\%$  of the total source flux. How do we explain the huge flaring of 4U 0115 +63? This X-ray binary consists of a neutron star spinning with 3.6 sec period and a  $\sim 10$  solar mass early type (B<sub>e</sub>) companion star orbiting around their common center of mass with 24.3 day period. Spectral type B<sub>e</sub> stars eject out a spherical shell of matter which flattens to a disk due to rapid rotation of the B<sub>e</sub> star. During its orbit when neutron star approaches closest to the B<sub>e</sub> star (called periastron passage) it

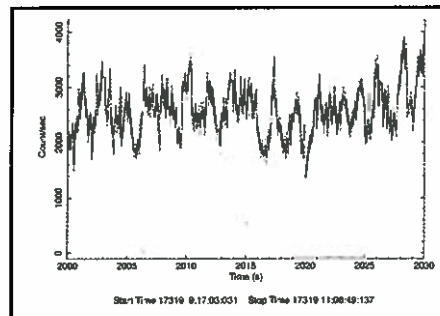


Fig. 23 : X-ray pulsations of 3.6 sec period are shown in this plot of count rate in 0.10 sec bins versus time for one of the LAXPCs (courtesy - LAXPC team).

crosses through the disk of the star resulting in sudden spurt in the rate of mass accretion on the neutron star. Since X-ray intensity is directly related to mass accretion rate, there is a type I X-ray outburst which lasts for a day. Type II bursts are rare and stronger and last for a few days.

In the PV phase LAXPC observed a Low Mass X-ray Binary (LMXB) known as 1728-34 and detected a thermonuclear X-ray burst shown in fig 24. The LMXBs have either a

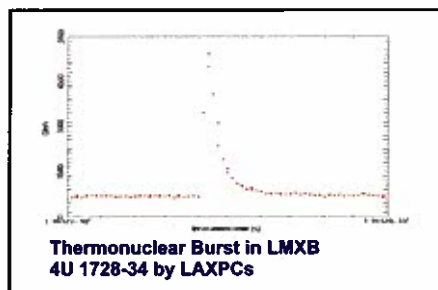


Fig. 24 : X-ray burst detected in the binary 4U 1728-34 with the LAXPC detectors. The bursts are a result of thermonuclear reaction ignited at a localized place on the surface of the neutron star (courtesy-LAXPC team).

neutron star or a black hole as the X-ray source and the companion star is  $\sim 1$  to 2 solar mass object. In LMXBs the neutron star has a magnetic field of  $\sim 10^9$  Gauss which is about 1000 times weaker than  $\sim 10^{12}$ - $10^{13}$  Gauss field for neutron stars in HMXBs. As a result, usually the accretion flow is

not channelled to the magnetic poles of the neutron star in LMXBs and hence usually LMXBs do not show X-ray pulsations. Note in the figure that the rise time of the burst is  $\sim$  a second and decay time is a few to ten seconds. What is the origin of the bursts? Detailed theoretical work that fits observed characteristics of the bursts, shows that the X-ray bursts arise due to ignition of thermonuclear reactions on the surface of the neutron star. The accretion is not homogeneous and uniform and matter piles up at localized regions. As more and more matter piles up, pressure and hence temperature increases and finally exceeds the ignition point of thermonuclear reactions. There is a huge thermonuclear explosion on a small part of the surface producing the X-ray burst. Initially the burst is localized but the flame of explosion spreads rapidly on the surface. As the neutron star is spinning rapidly, intensity oscillations at frequency of neutron star spin are produced in the decay phase of the burst. In the burst detected by the LAXPCs, QPOs (quasi-periodic oscillations) at 362 Hz are detected indicating neutron star spin period of 2.76 msec.

A High frequency (HF) QPO at 820 Hz shown in the power density spectrum is also detected in 4U 1728-34. There are several models to explain the HF QPOs. One model explains this as Keplerian velocity of temperature inhomogeneity in the high temperature gas in the innermost stable orbit around the neutron star.

Well known black hole binary Cyg X-1 was observed on October 23 and again on Oct 25, 2015. This bright object and many other black hole binaries show two states, a 'Soft' or 'High' state in which flux below 10 keV is high and the energy spectrum is soft and a 'Hard' or 'Low' state in which flux above 10 keV is high and the spectrum is hard.

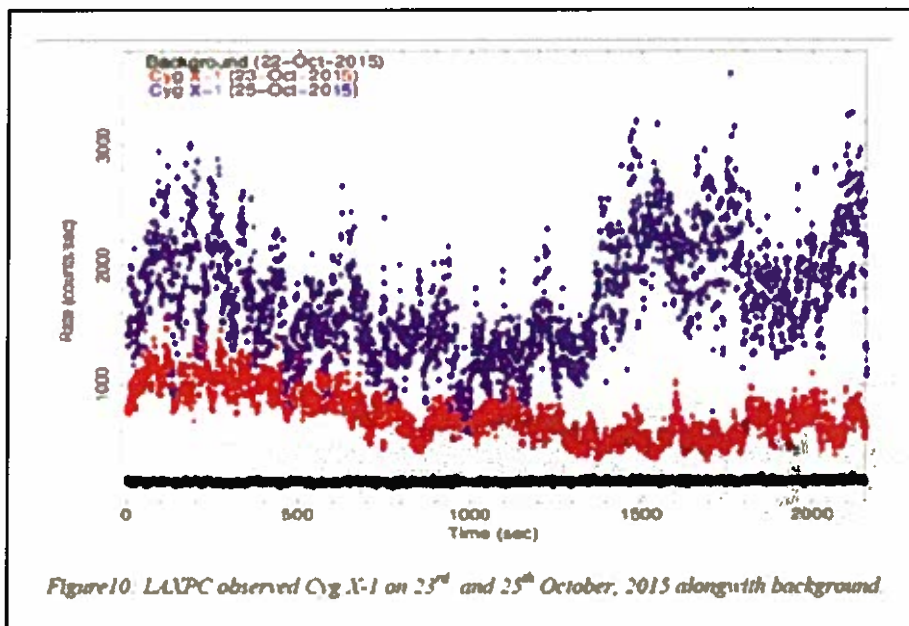


Fig. 25 : Two states of Cyg X-1 detected by LAXPC (courtesy - LAXPC team).

When first observed on October 23 the source was in a low state but it had made a transition to high state by October 25 as shown in fig 25. What triggers this state transition is still an unsolved puzzle. Chaotic intensity variations are quite pronounced and is an important feature of Cyg X-1.

Study of QPO and their characteristics at different energies is an important objective of LAXPC instrument. Most QPO studies have been at < 20 keV and there are few observations at higher energy. A transient black hole binary H 1743-322 was observed during its outburst. Its light curve shows randomly occurring intensity spikes. A power density spectrum of 30-80 keV light curve shown in fig 26 reveals presence of a strong QPO peak at ~0.6 Hz. This demonstrates sensitivity of LAXPC instrument for detecting QPOs at high energy. Detailed study of QPO characteristics like amplitude, width, Q-factor and their time lag with energy will be vital in understanding the origin of high energy QPOs.

These preliminary results from LAXPC instrument demonstrate its

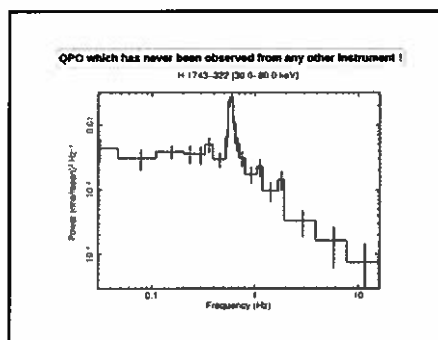


Fig. 26 : Detection of strong QPO at ~ 0.6 Hz in 30-80 keV from H 1743-322 (courtesy - LAXPC team).

sensitivity and potential for making new discoveries.

**(d) Preliminary results from UVIT:**

After opening the doors of the UVIT twin telescopes it has been tested and calibrated extensively by observing a variety of standard stars, UV bright stars, star clusters and galaxies. The tests done so far demonstrate that UVIT instrument is performing very well as per the design specifications. Plots showing angular response of UVIT in FUV and NUV channels are shown in fig 27 (a) and (b) from observation of open star cluster NGC 188. The derived values of ~ 1.2 and 1.6 arc sec demonstrate that the UVIT is performing better than its design

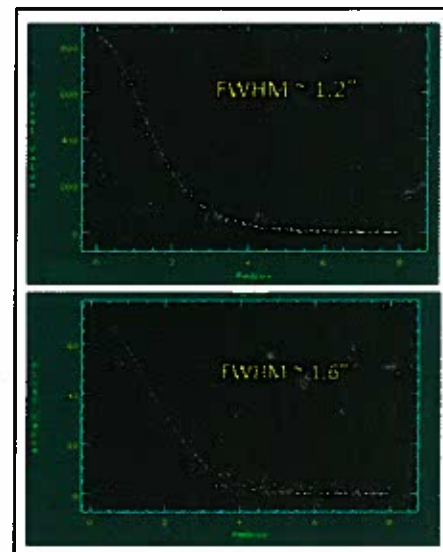


Fig 27 : (a) Angular resolution of NUV telescope of UVIT derived from observations of NGC 188 (b) same for the FUV telescope (courtesy: UVIT team).

goal of 1.8 arc A barred spiral galaxy NGC 2336 was observed by UVIT in PV phase and image in NUV band is shown in fig 28 along with image obtained by Galex and optical image from ground based telescope. Note that UVIT/ NUV image is much sharper compared to the Galex image resolving young hot stars and delineating the spiral structure of the galaxy clearly. UVIT/ FUV image is shown in fig 29. The superior angular resolution of UVIT is expected to make major contribution to morphological and structural studies of extended objects like galaxies, SNRs, novae, planetary nebulae etc. The UVIT can also obtain low resolution spectra in NUV and FUV bands by using gratings mounted in the filter wheels. Spectra of planetary nebula NGC 40 in the FUV band are shown in fig 30 and one can see the spectral lines clearly.

Data pipeline of UVIT is now almost ready and one can expected several new and interesting results from UVIT in coming months.

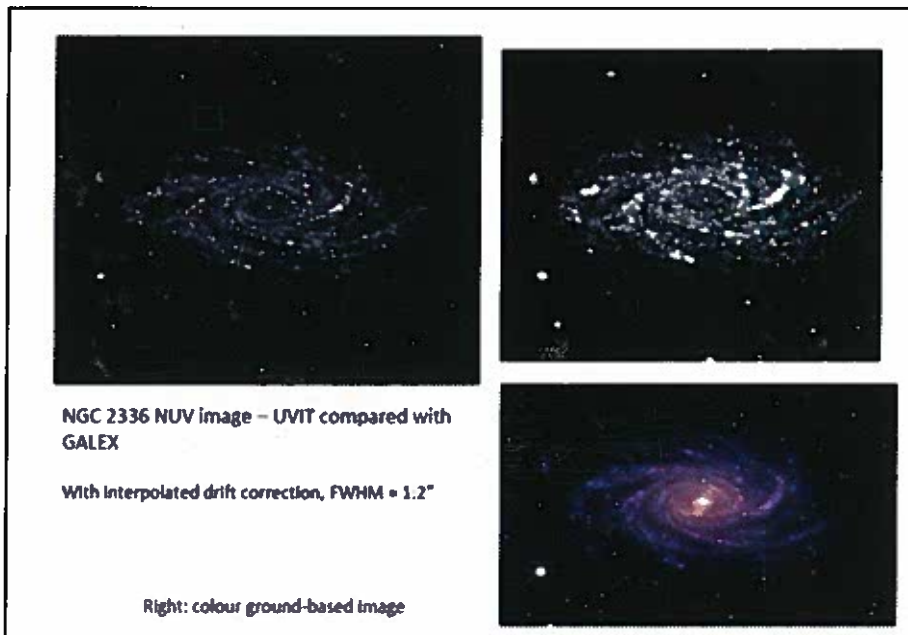


Fig. 28 : Images of barred spiral galaxy NGC 2336 (a) Left panel NUV image from UVIT (b) Right panel GaleX image (c) Optical image from ground based telescope (courtesy: UVIT team).



Fig 29: FUV image of galaxy NGC 2336 in CaF<sub>2</sub> filter (courtesy: UVIT team).

**Conclusion**

ASTROSAT mission took nearly 11 years to materialize and launch since the approval of the project by the government in 2004. The design and development of the 5 science instruments was a challenging job as several new technologies were required to be developed indigenously. Despite small size of the instrument teams, they were successful in overcoming the various technological challenges and developed the payloads meeting the design goals. The mission also required development of new sub-systems like attitude control system, phased array antenna etc which were

under the GT phase. Preliminary results from the instruments so far demonstrate that ASTROSAT has capability of achieving the science goals with which it was conceived and designed.

**Acknowledgement**

ASTROSAT was a combined national effort of ISAC and other ISRO centers as well as the instrument teams from various institutions. There are too many people to be named in this article who contributed to its completion and launch and I thank them for their dedication and perseverance. I express grateful thanks, on behalf of the instrument teams, to Dr K. Kasturirangan, then Chairman of ISRO, who has been very supportive of ASTROSAT right from its conception and successful

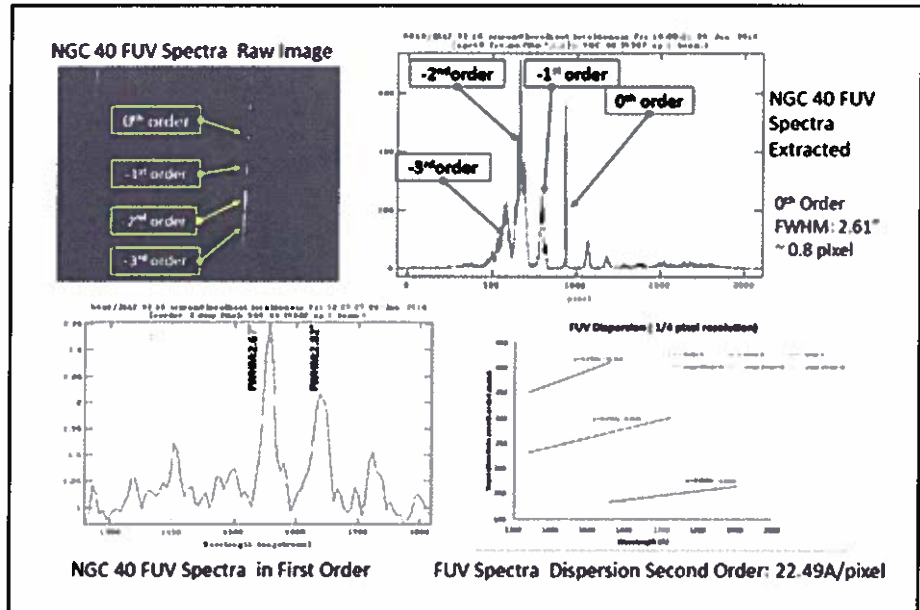


Fig. 30 : FUV spectra of NGC 40 obtained by UVIT (courtesy: UVIT team)

done successfully by the ASTROSAT project team. It is an internationally competitive mission which will place India at the forefront of research in high energy astronomy. Since its launch nearly 13 months ago, the ASTROSAT observatory has been functioning well and now making regular observations of sources proposed by the instrument teams

completion. Thanks are due to the successive Chairmen of ISRO and Directors of ISAC for their constant support of ASTROSAT. I also thank Shri V. Koteswararao, Project Director of ASTROSAT during 2003-2009 and his successor Shri Suryanarayan Sarma and the project team at ISAC for steering the project with great dedication leading to its successful

completion. I am grateful to Dr C.M. Ramadevi, Prof A.R. Rao, Prof K.P. Singh, Prof S.N. Tandon and Prof J. S. Yadav, the present PIs of SSM, CZTI, SXT, UVIT and LAXPC instruments respectively and their teams whose results I have presented in this article, for making ASTROSAT a success story. Finally, I thank Dr. S. Seetha, present PI of Astrosat for her contribution to Astrosat

**References**

[1] Agrawal, P.C. Adv. Space Res. 38, 2989A, 2006.

[2] Bowyer, C.S., Byram, E.T., Chubb, T.A. and Friedman, H. Science, 146, 912, 1964.

[3] Ghosh, P. and Lamb, F. ApJ 234, 296, 1979.

[4] Giacconi, G. and Rossi, B. J. of Geophys Res. 65, 773, 1960.

[5] Giacconi, G., Gursky, H., Paolini, F. and Rossi, B. Phys. Rev. Lett. 9, 439, 1962.

[6] Giacconi, G., Gursky, H., Kellog, E., Shereier, E. and Tanabaum, H. ApJ 167, L67, 1971.

[7] Paul, B, Agrawal, P. C., Rao, A., R., Vahia, M., Yadav, J., S., Seetha, S. and Kasturirangan, K. ApJ, 492, L63, 1998.

[8] Schreier, E., Levinson, R., Gursky, H., Kellog, E., Tananbaum, H. and Giacconi, G. ApJ 172, L79, 1972.

[9] Shakura, N.I. and Sunyaev, R. Astron. & Astrophys. 24, 337, 1973.

[10] Shklovasky, I. S. ApJ 148, L1, 1967.

[11] Singh, K.P., Tandon, S.N., Agrawal, P.C. etc., Proceedings of the SPIE, Volume 9144, id. 91441S 15 pp. (2014).

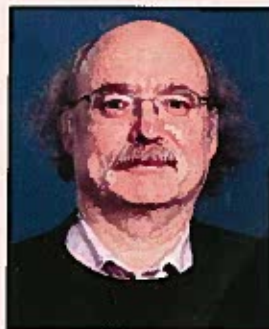
[12] Tanaka, Y., Nandra, K., Fabian, A.C., Inoue, H., Dotani, K., Hayashida, K., Iwasaka, K., Kuneida, K., Makino, F. and Matsuoka, M. Nature 375, 659, 1995.

[13] Trumper, J., Pietsch, W., Reppin, C., Voges, W., Staubert, R. and Kendziorra, E., ApJ 219, L105, 1978. van der Kliss, M. Proc National ASI 1997 (astro-ph 9710016).

**This year's Nobel Prize in Physics has been awarded to**



**David J. Thouless (b. 1934)**  
University of Washington, Seattle, WA, USA



**F. Duncan M. Haldane (b. 1951)**  
Princeton University, NJ, USA  
and



**J. Michael Kosterlitz (b. 1943)**  
Brown University, Providence, RI, USA

*"for theoretical discoveries of topological phase transitions and topological phases of matter"*

While Professor Thouless will get half the share of the Nobel Prize money, the other half will be equally shared by Professor Haldane and Professor Kosterlitz.